



UNIVERSITY OF LEEDS

This is a repository copy of *Styrene maleic-acid lipid particles (SMALPs) into detergent or amphipols: An exchange protocol for membrane protein characterisation*.

White Rose Research Online URL for this paper:
<http://eprints.whiterose.ac.uk/155882/>

Version: Accepted Version

Article:

Hesketh, SJ orcid.org/0000-0002-3107-8842, Klebl, DP, Higgins, AJ et al. (6 more authors) (2020) Styrene maleic-acid lipid particles (SMALPs) into detergent or amphipols: An exchange protocol for membrane protein characterisation. *Biochimica et Biophysica Acta (BBA) - Biomembranes*, 1862 (5). 183192. ISSN 0005-2736

<https://doi.org/10.1016/j.bbamem.2020.183192>

© 2020 Published by Elsevier B.V. This manuscript version is made available under the CC-BY-NC-ND 4.0 license <http://creativecommons.org/licenses/by-nc-nd/4.0/>.

Reuse

This article is distributed under the terms of the Creative Commons Attribution-NonCommercial-NoDerivs (CC BY-NC-ND) licence. This licence only allows you to download this work and share it with others as long as you credit the authors, but you can't change the article in any way or use it commercially. More information and the full terms of the licence here: <https://creativecommons.org/licenses/>

Takedown

If you consider content in White Rose Research Online to be in breach of UK law, please notify us by emailing eprints@whiterose.ac.uk including the URL of the record and the reason for the withdrawal request.



eprints@whiterose.ac.uk
<https://eprints.whiterose.ac.uk/>

Styrene maleic-acid lipid particles (SMALPs) into detergent or amphipols: An exchange protocol for membrane protein characterisation

Sophie J. Hesketh^{a,b}, David P. Klebl^{a,b}, Anna J. Higgins^{a,b}, Maren Thomsen^{a,b}, Isabelle B. Pickles^{b,c}, Frank Sobott^{b,d,e}, Asipu Sivaprasadarao^a, Vincent L.G. Postis^f & Stephen P. Muench^{a,b,*}

^a School of Biomedical Sciences, Faculty of Biological Sciences, University of Leeds, LS2 9JT, U.K.

^b Astbury Centre for Structural Molecular Biology, University of Leeds, LS2 9JT, U.K.

^c Department of Discovery and Translational Science, Leeds Institute of Cardiovascular and Metabolic Medicine, University of Leeds, Leeds LS2 9JT, U.K.

^d School of Molecular and Cellular Biology, Faculty of Biological Sciences, University of Leeds, LS2 9JT, U.K.

^e Department of Chemistry, Biomolecular & Analytical Mass Spectrometry group, University of Antwerp, 2020 Antwerpen, Belgium.

^f Biomedicine Research Group, Faculty of Health and Social Sciences, Leeds Beckett University, LS1 3HE, U.K.

*To whom correspondence should be addressed: Dr Stephen Muench, Faculty of Biological Sciences, University of Leeds, Leeds, LS2 9JT, U.K., (0113 343 4325) s.p.muench@leeds.ac.uk

Running title: SMALP exchange method into detergent and amphipol

Keywords: Membrane proteins, SMA co-polymer, SMALP, electron microscopy, mass spectrometry, amphipols.

Highlights:

- The first reported exchange protocol for transferring membrane proteins solubilised in SMALPs, into detergent or amphipols.
- Purification of protein:lipid complexes in the complete absence of detergent for use with native mass spectrometry and subsequent lipid identification.
- Cost effective membrane protein purification requiring minimal amounts of detergents, while increasing homogeneity of native lipid-protein complexes.

Abstract

Membrane proteins are traditionally extracted and purified in detergent for biochemical and structural characterisation. This process is often costly and laborious, and the stripping away of potentially stabilising lipids from the membrane protein of interest can have detrimental effects on protein integrity. Recently, styrene-maleic acid (SMA) co-polymers have started to address this issue, as they can extract membrane protein complexes directly from the membrane alongside their native lipid environment (SMALPs). However, their use is not without limitations. The inherent nature of the polymer renders SMALPs challenging for some downstream applications – such as mass spectrometry (MS), which is a powerful tool for examining membrane protein:lipid interactions. Whilst great progress has been made in the field of cryo-electron microscopy (EM), the resolution obtained is often insufficient to accurately identify closely associated lipids within the annulus. Native-MS has the potential to fill this knowledge gap, but the SMA polymer itself remains largely incompatible with this technique. To increase sample homogeneity and allow characterisation of membrane protein:lipid complexes by native-MS, we have developed a novel SMALP-exchange method; whereby the MP of interest is first solubilised and purified in SMALPs, then transferred into amphipols or detergents. This potentially allows endogenously associated lipids extracted by the SMA co-polymer to be identified and examined by MS, thereby complementing results obtained by cryo-EM and creating a better understanding of how the lipid bilayer directly affects membrane protein structure and function.

1. Introduction

Despite their physiological importance, our structural, biochemical and biophysical understanding of membrane proteins *in vivo* is limited. This is largely due to the challenges associated with their extraction and subsequent instability outside of their native lipid environment. Traditional *in vitro* membrane protein characterisation methods edict that the protein is extracted in detergent, which strips away the native membrane and encapsulates the hydrophobic transmembrane region within a micelle to keep it suspended in solution, often delipidating the membrane protein complex in the process. The detergent then remains present throughout all stages of the purification but can be later exchanged for a different detergent or a more suitable detergent system/solubilisation platform for downstream experimentation. However, this process is not trivial, and often much time, money and resources are committed to optimisation of solubilisation and purification conditions. A number of alternative reconstitution platforms have been developed to combat detergent-associated issues, such as membrane scaffold protein nanodiscs^{1,2}, amphipols^{3,4}, peptidiscs⁵, bicelles⁶ and liposomes⁷. However, all of these methods require an initial detergent solubilisation step, often resulting in reduced membrane protein activity and/or detrimental structural perturbations⁸⁻¹².

In an attempt to overcome these issues entirely, styrene-maleic acid (SMA) lipid particles (SMALPs) were developed as a platform for membrane protein solubilisation¹³⁻¹⁶. SMA co-polymers act by solubilising membrane proteins directly from the membrane while retaining their native lipid environment^{13,15-17}. The SMALP:membrane protein complexes remain intact throughout the purification process, from the initial solubilisation stage through to storage¹¹. Moreover, the SMA co-polymer can be easily synthesised in-house by hydrolysis of its precursor anhydride, SMA2000¹⁶. This offers a significant advantage over conventional detergents, as it enables solubilisation of a more challenging range of the membrane proteins - such as large complexes with highly integrated lipid structures - but at a significantly reduced cost. However, SMALPs are not without limitations and are sensitive to low pH (<6.5) and the presence of divalent cations (> 5 mM)^{16,18,19}. This is a limitation for a number of downstream applications which have particular constraints on buffer composition, such as functional assays and structural techniques including mass spectrometry (MS) and electron microscopy (EM)^{20,21}. Derivatives of SMA and alternative co-polymers have been designed to overcome issues with sample heterogeneity²², and susceptibility to pH and divalent cations^{19,23,24}, but as of yet no one-size-fits-all solution has been established.

We thus propose a more combinatorial approach to *in vitro* membrane protein characterisation, whereby the membrane protein of interest is first extracted in SMALPs, and subsequently exchanged into a more appropriate system for downstream applications. In this context, SMALPs act as a powerful tool for initial solubilisation and purification of membrane proteins, offering a significantly cheaper, stable alternative to conventional detergent purification methods, while retaining lipids from the membrane proteins native environment.

2. Materials and Methods

2.1 *AcrB* expression, solubilisation and purification

The styrene-maleic acid (SMA) co-polymer (SMA2000, Cray Valley – now trading under Polyscience, N.L) was hydrolysed in-house and stored at 4 °C as a powder stock, as described previously¹⁶. *Escherichia coli* (*E. coli*) AcrB(His)₈ was expressed and purified with 2.5 % (w/v) SMA as described previously²⁵, albeit with a few modifications. Briefly, the C43(DE3), pRARE2, ΔacrB strain of *E. coli* was used for overexpression by auto-induction in SB media²⁶. Cell membranes were prepared as described in²⁷, and the membrane pellet was resuspended in a minimal volume of binding buffer (BB: 500 mM NaCl, 10 % glycerol, 50 mM Tris-HCl, pH 8.0) before snap-freezing in liquid nitrogen. The PierceTM BCA protein assay kit (ThermoScientific, U.K.), was used to estimate protein concentration in the isolated membranes. For solubilisation in SMA, membranes were weighed to give ~45 mg total protein and resuspended in BB to an equivalent concentration of 1 mg/ml of protein. SMA co-polymer was added to a final concentration of 2.5 % (w/v), and the mixture was incubated for 2 hours at room temperature with inversion. AcrB purified in n-dodecyl-β-D-maltoside (DDM:AcrB) was solubilised in BB plus 1 % DDM and incubated at 4 °C for 2 hours. Insoluble material was pelleted by centrifugation at 100,000 $\times g_{av}$, 4 °C, and the soluble fractions were incubated with pre-equilibrated HisPurTM cobalt resin (ThermoScientificTM, U.K.) overnight at 4 °C. To purify the protein, the resin was first washed with 10 column volumes (CV) of BB (plus 0.025 % DDM for DDM:AcrB; DBB), then 10 CV of BB (or DBB) supplemented with 20 mM imidazole, before eluting in 1 ml fractions with elution buffer (BB or DBB plus 300 mM imidazole). Fractions containing the eluted protein (identified by SDS-PAGE) were pooled and dialysed into BB or DBB and then concentrated using an Amicon Ultra 100 kDa MWCO centrifugal filter (Merck Millipore, U.K.), before being snap-frozen in small volumes and stored at -80 °C.

2.2 SMA-exchange procedure

For amphipol exchange, A8-35 (5 % w/v in H₂O) was added to SMA-purified AcrB (~0.5 mg/ml for routine exchange, and up to 4.5 mg/mL for SEC-MALLS analysis), 3:1 w/w amphipol:protein ratio and incubated on ice for 30 minutes. For detergent exchange, a final concentration of 1 % n-dodecyl-β-D-maltoside (DDM) was added to the purified protein sample instead. All sample volumes were ~200 μL or less. After this incubation, the exchange samples and A8-35/DDM-free controls were treated with incremental concentrations (0.5, 1.0, 1.5 and 2.0 mM) of MgCl₂ to precipitate SMA. Thus, MgCl₂ was first added to give a final concentration of 0.5 mM, incubated at 4 °C for 1 hour with gentle inversion, and then centrifuged at 100,000 $\times g_{av}$, 4 °C, for 1 hour. The supernatants were transferred to fresh microfuge tubes, and 2 μl aliquots were taken for detection of AcrB(His)₈ by dot blot. Incubation with MgCl₂ and subsequent centrifugation steps were repeated four times in total, until the final MgCl₂ concentration reached 2 mM. The A8-35 MgCl₂-free controls were also subject to the same periods of incubation and centrifugation for consistency. The final product was taken for further analysis by SEC-MALLS, negative stain electron microscopy, and mass spectrometry. Samples were exchanged into the appropriate buffers for each application before use.

2.3 Dot blot

Supernatant samples were mixed 1:1 (v/v) with 0.1 % SDS and 25 mM DTT and incubated at room temperature for a minimum of 5 minutes. Samples were spotted directly onto nitrocellulose membranes (0.45 μ m pore size) in a 2 μ L volume and left to air-dry. Blots were blocked with 5 % Marvel milk in PBST (13.7 mM NaCl, 0.27 mM KCl, 1 mM Na₂HPO₄·7H₂O, 0.18 mM KH₂PO₄ and 0.05 % Tween 20), for 1 hour at room temperature. Membranes were rinsed twice in PBST for 5 minutes, before submerging in 2 % Marvel milk in PBST supplemented with 1:4000 diluted HRP-conjugated monoclonal mouse anti-His antibody (R&D Systems, U.K.) for a further 1 hour at room temperature. Blots were then washed for 1 hour with PBST before developing.

2.4 Size exclusion chromatography with multi-angle laser light scattering (SEC-MALLS).

SMA:AcrB and A8-35 exchanged (A8-35_Ex) samples were dialysed into 300 mM NaCl, 50 mM Tris-HCl, pH 8.0 (SECB) prior to SEC-MALLS experimentation. DDM exchanged (DDM_Ex) samples were dialysed into SECB plus 10 % glycerol and 0.025 % DDM (DDM-SECB) to decrease the DDM concentration. For the protein-free lipid particles, 5 mg of *E. coli* total lipid extracts (Avanti Polar Lipids Inc., U.S.A.) were suspended by sonication in SECB, and split into two for the addition of 2.5 % SMA and 2.5 % A8-35. SEC-MALLS experiments were performed using a Superose 6 5/150 column pre-equilibrated with SECB for SMA:AcrB and A8-35_Ex samples, and DDM-SECB without glycerol for DDM-containing samples. The data were collected on a DAWN 8+ multi-angle light scattering (LS) detector, an Optilab T-rEX differential refractive index (dRI) detector and UV-absorbance (UV) detector (Wyatt Technology), and samples were run at a flow rate of 0.2 mL/minute. Astra 6.2 software was implemented for molar mass calculations. The absorbance value at 0.1 % OD_{280nm} for full-length AcrB(His)₈ was given as 0.79 g/L and a refractive index increment (dn/dc) value of 0.185 mL/g was applied to the protein component - AcrB. A8-35 and DDM dn/dc modifiers were set at 0.15 and 0.143, respectively, for the surfactant components.

2.5 Negative stain electron microscopy

Negative stain grids were prepared and examined as previously described²⁰. Briefly, in-house carbon-coated copper grids were glow-discharged (PELCO easiGlow, TedPella) for 30 s. 3 μ L of sample at a concentration of ~20 μ g/mL was then applied to the grid for 30 s and blotted before staining twice with 1% uranyl acetate (2x 30s). Micrographs were collected using a Tecnai F20 microscope fitted with a 4k x 4K CMOS camera, operating at 200 kV with a nominal magnification of 50,000X ($\text{\AA}/\text{pix} = 2.0$).

2.6 Lipid extraction and denaturing mass spectrometry

Lipid extraction was performed as described in²⁸, albeit with the following modifications. All steps of lipid extraction were performed on ice or at 4 °C. To 40 μ L A8-35_Ex (1 volume; [AcrB] ~1.5 mg/mL), 1 volume of chloroform and 2 volumes of methanol were added. The sample was mixed and another volume of chloroform was added. After mixing again, 1 volume of water was added. The sample was centrifuged (7 min, 17,000 xg), before the organic phase

was washed three times with 2 volumes of cold water. The organic phase was directly analysed by nano-electrospray ionisation (nESI)-MS using in-house coated gold/palladium nanospray capillaries and a quadrupole time-of-flight MS (Synapt G1 HDMS, Waters) operating in negative mode. For denaturing MS of lipid extracts, the synapt was operated with the following parameters: Capillary voltage = 1.2 kV, source temperature = 80 °C; sampling cone = 80 V; extraction cone = 4 V; backing pressure = 2 mbar; trap collision energy (CE) = 20 V; trap flow rate = 2 mL/min, transfer CE = 10 V and trap DC bias = 4. The most intense signal (719 m/z) was selected and fragmented by MS/MS under the same conditions, except with trap CE = 50 V.

2.7 Native mass spectrometry

Samples were prepared for MS by diluting with 200 mM ammonium acetate, pH 7.4, and re-concentrating with an Amicon Ultra 0.5 mL (100 kDa MWCO) concentrator. This was repeated at least three times to ensure buffer exchange. Native MS was also done using nESI with in-house prepared nanospray capillaries on a Synapt G1, operated in positive ion mode. The instrument parameters were as follows: Capillary voltage = 2.0 kV; source temperature = 80 °C; sampling cone = 180 V; extraction cone = 4 V; backing pressure = 6 mbar; trap CE = 220 V; transfer CE = 200 V and trap DC bias = 4. All MS data were analysed with MassLynx software (Waters).

3. Results and Discussion

3.1 SMA-exchange procedure

The SMA-exchange procedure was designed to capitalise on the polymers' inherent sensitivity to divalent cations, whereby MgCl₂ was used to gradually destabilise the SMA polymer and thus promote protein incorporation into an alternative platform – such as detergent or another amphipathic polymer. The *E. coli* multidrug efflux pump, acridine resistance protein B (AcrB), was chosen as a model system to test the exchange, as it has been previously characterised by a variety of biochemical and biophysical techniques in detergents^{29,30}, amphipols³¹ and SMALPs^{25,32}.

AcrB was extracted and purified in SMALPs (SMA:AcrB) using a one-step IMAC cobalt purification, as previously described²⁵. Purification was also performed in n-dodecyl-β-D-maltoside (DDM) for comparison (DDM:AcrB) (Figure 1A and B). AcrB purified using the SMA co-polymer routinely yielded a purer sample in the elution fractions, thus limiting the number of downstream steps required to purify the sample further. This prevents unnecessary protein loss as a result of additional purification steps, which in turn increases cost-effectiveness.

To destabilise SMA:AcrB and encourage exchange, the purified sample was first dialysed into BB, then incubated with (0.5 mM) MgCl₂ for 1 hour in the presence or absence of either amphipol A8-35 (A8-35) or DDM. Although it has been shown that amphipols are also sensitive to divalent cations, they are relatively more tolerant to Mg²⁺ than the SMA co-polymer, which starts to heavily precipitate at 2 mM MgCl₂ in this instance (Figure 1C)^{19,33}. It is likely that using an alternative amphipathic polymer or detergent (e.g DDM) which is less

sensitive to divalent cations would perform better in the exchange than the A8-35 amphipol polymer tested here. Alternatively, a polymer variant that is more sensitive to divalent cations, such as SMA3000, may increase the efficiency of the exchange process³⁴. After the first incubation with 0.5 mM MgCl₂, insoluble material was pelleted by centrifugation at 100,000 xg, before increasing the MgCl₂ concentration by a further 0.5 mM and incubating for another hour. These steps were repeated until the mixture reached a final concentration of 2 mM MgCl₂. Dot blots were used to monitor the quantity of soluble AcrB remaining in the supernatant throughout the exchange process with the aim of keeping sample use to a minimum (Figure 1C), but for clarity the A8-35 exchange samples were also analysed by standard western blotting (Supplementary Figure 1E).

The dot blot showed that AcrB remains in the soluble fraction at 2 mM concentrations of MgCl₂ when in the presence of A8-35 or DDM, but completely precipitates in the absence of such a rescue agent (Figure 1C). A MgCl₂-free control was also included to examine the effect of the competing A8-35 polymer alone (Figure 1C, +A8-35). The final protein concentration in the +A8-35 samples is similar to that of the exchanged sample (Supplementary Table 1), suggesting that the presence of a rescue agent alone does not destabilise the AcrB-SMA complex and cause precipitation. There is sample loss during the exchange process which is also commonly seen when conducting detergent exchange also. However, as the goal of the exchange is to remove the SMA copolymer, the presence of MgCl₂ as a precipitant is necessary to assist in exchange efficiency. It is also noteworthy that the nature of the transmembrane annulus after addition of the exchange material in the presence or absence of MgCl₂ – whether a complete exchange has occurred, or a polymer/detergent hybrid has formed – is unknown. In future, although beyond the scope of this study, the use of fluorescently labelled SMA and amphipols could be used to quantitatively determine the exchange efficiency and give more insight into the true amount of remaining SMA polymer^{35,36}. Additionally, while the MgCl₂ concentration used here has been shown to precipitate the polymer and the associated protein out of solution (Figure 1C, +MgCl₂), and it has been shown that the sensitivity to divalent cations is polymer-specific³⁷, the required concentration for precipitation is likely to be protein dependent and should be empirically determined for different systems. It is also noteworthy that the volume of the reaction and concentration of the protein may play a role in exchange efficiency, and these experiments were designed with low protein concentrations in ~200 µl volumes in mind.

3.2 Validation of exchange and examining polymer influence with SEC-MALLS

SMA co-polymers have an average polydispersity index of ~2.6^{38,39}. This polymer heterogeneity makes the membrane protein-SMA particle characterisation difficult, particularly when used in conjunction with techniques that prioritise sample homogeneity²³. There have been attempts to decrease the heterogeneity of the polymer by altering the synthesis procedure and polymer length, but it has been suggested that the SMA co-polymer's solubilisation efficiency is owed to this heterogeneity⁴⁰. This protocol was therefore designed to reduce sample heterogeneity without interfering with the original polymer synthesis procedure.

To examine the effect that SMA and A8-35 can have on the polydispersity of a sample, protein-free SMA lipid particles (SMA_LP) and A8-35 lipid particles (A8-35_LP) were examined by size exclusion chromatography with multi-angle laser light scattering (SEC-MALLS), and their

absorbance was monitored across multiple wavelengths (Figure 2A and 2B). SMA_LP significantly absorbed in the UV spectrum from ~200-270 nm, with a gradual drop in absorbance before 280 nm. The SMA_LP also eluted slowly from the SEC column, visualised as a broad primary elution peak spanning >5 minutes of the total 20-minute run. The A8-35_LP did not display similar characteristics, and instead eluted in a sharper peak spanning ~2.5 minutes of retention time. This highlights a possible advantage of using amphipols as a homogeneous tool instead of SMA for techniques such as MS. The absorbance spectra of SMA_LPs, A8-35_LPs were measured alongside DDM and a DDM-A8-35 mix in triplicate to validate these absorbance readings (Figure 2C).

Exchanged AcrB samples were also analysed by SEC-MALLS to determine whether sample homogeneity had improved. Comparison of the SEC-MALLS chromatograms of SMA:AcrB and the A8-35 exchanged (A8-35_Ex) sample showed a reduction in heterogeneity between the starting material and final exchanged product, indicated by a leading trail before the primary elution peak for SMA:AcrB, and a sharp elution peak for A8-35_Ex at ~10 minutes (Figure 2D and 2E); and is further demonstrated by a more consistent molar mass distribution of A8-35_Ex across this peak (Figure 2D, Supplementary Figure 2A). Aggregates of high laser light scattering (LLS; Figure 2E) and low UV absorbance were also observed in the void volume for the SMA:AcrB sample, potentially indicating the presence of polymer-only aggregates. No such aggregation was observed in the void volume for A8-35_Ex, but a large LLS peak corresponding to the size of empty A8-35 lipid particles was consistently observed after the exchange at an elution time of ~11.35 min⁴¹ (Figure 2B and 3E). Accurate molar masses could not be determined for SMA:AcrB due to discrepancy in the literature describing the refractive index increment (dn/dc) for SMA co-polymers^{15,22,34}, but a dn/dc polymer modifier of 0.15⁴¹ could be applied to the A8-35 sample to give an estimated molar mass of ~450 kDa at the highest peak (Figure 2A and Supplementary Figure 2A). Analytical ultracentrifugation has previously determined the molecular mass of AcrB in SMA to be >400 kDa⁴², although it has been observed at variable molecular weights ranging from its native ~340 kDa up to and exceeding 800 kDa^{42,43}.

AcrB was also exchanged into DDM (DDM_Ex) and analysed alongside a control sample that had been solubilised and purified in DDM by conventional methods (Figure 1A, supplementary figure 1B). No significant aggregation was observed in the SEC-MALLS elution profile of either sample. The DDM_Ex elution peak also has a slight decrease in retention time (~ 10.2 min) compared to the DDM purified sample (~10.4 min, supplementary information). Despite this peak shift, the primary elution peak for DDM_Ex at 10 minutes is still less broad. However, a modifier dn/dc value of 0.143, corresponding to the DDM micelle RI, was applied to both samples, and gave a similar molar mass distribution (~400 kDa) to the A8-35_Ex sample. The molar mass distribution shows a homogeneous mixture at this point and the reason for this is unclear but could again be due to the unclear nature of the lipid annulus.

3.3 Validation of Exchange: Negative Stain Microscopy

Negative stain microscopy was used to visually assess the homogeneity and integrity of the exchanged samples vs the progenitor SMA:AcrB sample (Figure 3). Both DDM_Ex and A8-35_Ex were monodisperse and homogeneous on the grid, and particles clearly maintained the

characteristic AcrB architecture, which is typically seen as a broadly triangular in shape^{29,32,44}. Although negative stain can report on the overall quality of the protein sample in terms of aggregation and degradation, the resolution is not sufficient to see subtle changes in structure or discern the nature and lipid content of the annulus surrounding the protein of interest.

3.4 Validation of exchange: Mass Spectrometry

One significant advantage of adopting a SMALP method is that it can extract and isolate the protein of interest in the presence of its native lipid annulus^{13,15–17}. Recently, MS has emerged as a powerful complementary tool for examining these extracted membrane protein:lipid complexes, both in native-MS to determine lipid stoichiometry^{12,45,46}, and LC-MS/MS to examine their lipid profile^{43,47}. However, the heterogeneity of the SMA polymer and its inability to dissociate easily in the gas phase has proved problematic for native-MS studies of SMA:membrane protein complexes, as the SMA co-polymer produces a large variety of charge states with complex drift time measurements. Exchanging the bound SMA with a detergent or amphipol may overcome this issue, as both amphipols^{48,49} and detergents^{45,50} have been extensively characterised in MS^{51,52}. It has also been previously shown that A8-35:membrane protein complexes out-perform their detergent counterparts, so it would be beneficial for the membrane protein to have been fully exchanged into this system⁵³. Additionally, subsequent lipidomic assessment of A8-35_Ex and DDM_Ex samples would complement native-MS results. To this end, we compared A8-35_Ex and DDM_Ex in native MS to first examine the complexes individually, and then used tandem mass spectrometry (MS/MS) to identify the presence of any remaining lipids.

MS analysis showed that the exchange of the protein from SMA to both A8-35 and DDM was achieved to some degree, as firstly, spectra had been observed where this was not previously obtainable for SMA:AcrB; secondly, the observed spectra are similar to that of the published detergent:AcrB spectrum⁵⁰ (Figure 4A and B). These traces were of low resolution, even at high collision energies, which may suggest that a small amount of SMA co-polymer remains bound but overall demonstrate that a more homogeneous, tractable sample had been generated.

Based on previous evidence of lipid retention in SMA^{23,47}, we also hypothesised that native lipids were carried through during the transfer from SMA:AcrB to A8-35_Ex, as the protein was not initially extracted in delipidating conditions. DDM is known to delipidate membrane proteins for mass spectrometry, but this information is not available for amphipols⁴⁵. After the exchange, lipids of the non-detergent exposed A8-35_Ex sample were extracted and the crude extract directly subjected to MS analysis. The resulting spectra show a large number of putative lipid peaks. The most intense peak at $m/z = 719.5$ was taken forward to tandem MS and assigned to phosphatidylglycerol (16:0/16:1) according to previously published data⁵⁴. This was further validated using LIPID MAPS glycerophospholipid MS/MS prediction⁵⁵ (Figure 4C). Albeit a very preliminary result, this shows that lipids can be retained through this entirely detergent free purification and exchange procedure and provides a base for future investigation into how the relationship between solubilising agent (polymer/detergent) can define the nature of the lipid annulus, and thus how membrane proteins interact with their native bilayer.

4. Conclusions

Here, we present a method of platform exchange for membrane proteins, purified with the SMA co-polymer, to enhance compatibility with downstream applications, such as MS, EM and SEC. The method capitalises on the ability of $MgCl_2$ to precipitate out the SMA co-polymer, in the presence of an alternative solubilisation platform, such as detergents or amphipols. A further advantage is that it allows native lipids to be carried through the initial protein solubilisation/purification steps, which enhances the stability of the membrane protein in solution. Additionally, as detergents and amphipols are not required in the membrane protein preparation until the final exchange step, it can significantly reduce the costs commonly associated with standard detergent purifications. AcrB was used as a model system to test the exchange process, as it is extensively characterised in a number of reconstitution platforms. To this end, we successfully purified AcrB with the SMA co-polymer and exchanged the polymer for an alternative platform – namely, amphipol, A8-35 and detergent, DDM. The final exchange product was more homogeneous, could withstand millimolar concentrations of $MgCl_2$ and gave observable spectra in native-MS analysis, which were our initial objectives. The exchange process can also be performed on a small scale with minimal sample loss, which is beneficial to more difficult systems where low protein concentrations are obtained. We also were able to use mass spectrometry to present evidence that lipids are carried over from the transfer of SMA into A8-35, which opens up the possibility of analysing native membrane protein:lipid complexes extracted and purified in the complete absence of detergent alongside a complimentary lipid profiles. Overall this method has the potential to provide further insights into native membrane protein:lipid interactions by adding to the ever-expanding SMA toolbox for membrane protein characterisation (Figure 5).

5. Acknowledgments

We acknowledge the facilities of the Astbury Centre for Structural and Molecular Biology with the EM and Mass spectrometry facilities being supported by the University of Leeds and Wellcome Trust (108466/Z/15/Z & 208385/Z/17/Z). S.J.H. was supported by a Biotechnology and Biological Sciences Research Council (BBSRC) White Rose Doctoral Training Fellowship. I.B.P. was supported by a Wellcome Trust PhD scholarship (102174/B/13/Z). This work was supported by the BBSRC grant number BB/R018561/1.

6. References

1. Civjan, N. R., Bayburt, T. H., Schuler, M. A. & Sligar, S. G. Direct solubilization of heterologously expressed membrane proteins by incorporation into nanoscale lipid bilayers. *Biotechniques* **35**, 556–563 (2003).
2. Ritchie, T. K. *et al.* Chapter 11 - Reconstitution of membrane proteins in phospholipid bilayer nanodiscs. *Methods Enzymol.* **464**, 211–31 (2009).
3. Tribet, C., Audebert, R. & Popot, J.-L. Amphipols: Polymers that keep membrane proteins soluble in aqueous solutions. *Proc. Natl. Acad. Sci.* **93**, 15047–15050 (1996).
4. Zoonens, M. & Popot, J. L. Amphipols for Each Season. *J. Membr. Biol.* **247**, 759–796 (2014).

5. Carlson, M. L. *et al.* The Peptidisc, a simple method for stabilizing membrane proteins in detergent-free solution. *Elife* **7**, (2018).
6. Dürr, U. H. N., Gildenberg, M. & Ramamoorthy, A. The Magic of Bicelles Lights Up Membrane Protein Structure. *Chem. Rev.* **112**, 6054–6074 (2012).
7. Rigaud, J.-L., Pitard, B. & Levy, D. Reconstitution of membrane proteins into liposomes: application to energy-transducing membrane proteins. *Biochim. Biophys. Acta - Bioenerg.* **1231**, 223–246 (1995).
8. Dörr, J. M. *et al.* Detergent-free isolation, characterization, and functional reconstitution of a tetrameric K⁺ channel: The power of native nanodiscs. *Proc. Natl. Acad. Sci.* **111**, 18607–18612 (2014).
9. Seddon, A. M., Curnow, P. & Booth, P. J. Membrane proteins, lipids and detergents: Not just a soap opera. *Biochimica et Biophysica Acta - Biomembranes* **1666**, 105–117 (2004).
10. Reading, E. *et al.* The Effect of Detergent, Temperature, and Lipid on the Oligomeric State of MscL Constructs: Insights from Mass Spectrometry. *Chem. Biol.* **22**, 593–603 (2015).
11. Jamshad, M. *et al.* G-protein coupled receptor solubilization and purification for biophysical analysis and functional studies, in the total absence of detergent. *Biosci. Rep.* **35**, 1–10 (2015).
12. Gupta, K. *et al.* The role of interfacial lipids in stabilizing membrane protein oligomers. *Nature* **541**, 421–424 (2017).
13. Knowles, T. J. *et al.* Membrane Proteins Solubilized Intact in Lipid Containing Nanoparticles Bounded by Styrene Maleic Acid Copolymer. *J. Am. Chem. Soc.* **131**, 7484–7485 (2009).
14. Orwick-Rydmark, M. *et al.* Detergent-free incorporation of a seven-transmembrane receptor protein into nanosized bilayer lipodisc particles for functional and biophysical studies. *Nano Lett.* **12**, 4687–4692 (2012).
15. Jamshad, M. *et al.* Structural analysis of a nanoparticle containing a lipid bilayer used for detergent-free extraction of membrane proteins. *Nano Res.* **8**, 774–789 (2015).
16. Lee, S. C. *et al.* A method for detergent-free isolation of membrane proteins in their local lipid environment. *Nat. Protoc.* **11**, 1149–1162 (2016).
17. Scheidelaar, S. *et al.* Molecular model for the solubilization of membranes into nanodisks by styrene maleic Acid copolymers. *Biophys. J.* **108**, 279–90 (2015).
18. Dörr, J. M. *et al.* The styrene–maleic acid copolymer: a versatile tool in membrane research. *Eur. Biophys. J.* **45**, 3–21 (2016).
19. Fiori, M. C., Jiang, Y., Altenberg, G. A. & Liang, H. Polymer-encased nanodiscs with improved buffer compatibility. *Sci. Rep.* **7**, 7432 (2017).
20. Thompson, R. F., Walker, M., Siebert, C. A. & Ranson, N. A. An introduction to sample preparation and imaging by cryo-electron microscopy for structural biology. *Methods* **100**, 3–15 (2016).
21. Hernández, H. & Robinson, C. V. Determining the stoichiometry and interactions of macromolecular assemblies from mass spectrometry. *Nat. Protoc.* **2**, 715–726 (2007).
22. Domínguez Pardo, J. J. *et al.* Membrane Solubilization by Styrene-Maleic Acid Copolymers: Delineating the Role of Polymer Length. *Biophys. J.* **115**, 129–138 (2018).
23. Oluwole, A. O. *et al.* Solubilization of Membrane Proteins into Functional Lipid-Bilayer Nanodiscs Using a Diisobutylene/Maleic Acid Copolymer. *Angew. Chemie Int. Ed.* **56**, 1919–1924 (2017).

24. Hall, S. C. L. *et al.* An acid-compatible co-polymer for the solubilization of membranes and proteins into lipid bilayer-containing nanoparticles. *Nanoscale* **10**, 10609–10619 (2018).
25. Postis, V. *et al.* The use of SMALPs as a novel membrane protein scaffold for structure study by negative stain electron microscopy. *Biochim. Biophys. Acta - Biomembr.* **1848**, 496–501 (2015).
26. Glover, C. A. P. *et al.* AcrB contamination in 2-D crystallization of membrane proteins: Lessons from a sodium channel and a putative monovalent cation/proton antiporter. *J. Struct. Biol.* **176**, 419–424 (2011).
27. Postis, V. G. L., Rawlings, A. E., Lesiuk, A. & Baldwin, S. A. Use of Escherichia coli for the Production and Purification of Membrane Proteins. in 33–54 (2013). doi:10.1007/978-1-62703-351-0_3
28. Smirnova, I. A., Ädelroth, P. & Brzezinski, P. Extraction and liposome reconstitution of membrane proteins with their native lipids without the use of detergents. *Sci. Rep.* **8**, 14950 (2018).
29. Murakami, S., Nakashima, R., Yamashita, E. & Yamaguchi, A. Crystal structure of bacterial multidrug efflux transporter AcrB. *Nature* **419**, 587–593 (2002).
30. Du, D. *et al.* Structure of the AcrAB–TolC multidrug efflux pump. *Nature* **509**, 512–515 (2014).
31. Wang, Z. *et al.* An allosteric transport mechanism for the AcrAB-TolC multidrug efflux pump. *Elife* **6**, (2017).
32. Parmar, M. *et al.* Using a SMALP platform to determine a sub-nm single particle cryo-EM membrane protein structure. *Biochim. Biophys. Acta - Biomembr.* **1860**, 378–383 (2018).
33. Popot, J.-L. *et al.* Amphipols From A to Z*. *Annu. Rev. Biophys.* **40**, 379–408 (2011).
34. Morrison, K. A. *et al.* Membrane protein extraction and purification using styrene-maleic acid (SMA) copolymer: effect of variations in polymer structure. *Biochem. J.* **473**, 4349–4360 (2016).
35. Della Pia, E. A., Hansen, R. W., Zoonens, M. & Martinez, K. L. Functionalized Amphipols: A Versatile Toolbox Suitable for Applications of Membrane Proteins in Synthetic Biology. *J. Membr. Biol.* **247**, 815–826 (2014).
36. Lindhoud, S., Carvalho, V., Pronk, J. W. & Aubin-Tam, M.-E. SMA-SH: Modified Styrene–Maleic Acid Copolymer for Functionalization of Lipid Nanodiscs. *Biomacromolecules* **17**, 1516–1522 (2016).
37. Gulamhussein, A. A. *et al.* Examining the stability of membrane proteins within SMALPs. *Eur. Polym. J.* **112**, 120–125 (2019).
38. Grethen, A., Oluwole, A. O., Danielczak, B., Vargas, C. & Keller, S. Thermodynamics of nanodisc formation mediated by styrene/maleic acid (2:1) copolymer. *Sci. Rep.* **7**, 11517 (2017).
39. SMA Technical Documentation. (2016). Available at: [http://www.crayvalley.com/docs/technical-paper/sma-multi-functional-resins-\(europe\).pdf](http://www.crayvalley.com/docs/technical-paper/sma-multi-functional-resins-(europe).pdf).
40. Craig, A. F. *et al.* Tuning the size of styrene-maleic acid copolymer-lipid nanoparticles (SMALPs) using RAFT polymerization for biophysical studies. *Biochim. Biophys. Acta - Biomembr.* **1858**, 2931–2939 (2016).
41. Gohon, Y. *et al.* Well-defined nanoparticles formed by hydrophobic assembly of a short and polydisperse random terpolymer, amphipol A8-35. *Langmuir* (2006). doi:10.1021/la052243g

42. Postis, V. *et al.* The use of SMALPs as a novel membrane protein scaffold for structure study by negative stain electron microscopy. *Biochim. Biophys. Acta - Biomembr.* **1848**, 496–501 (2015).
43. Pollock, N. L. *et al.* SMA-PAGE: A new method to examine complexes of membrane proteins using SMALP nano-encapsulation and native gel electrophoresis. *Biochim. Biophys. Acta - Biomembr.* **1861**, 1437–1445 (2019).
44. Du, D. *et al.* Structure of the AcrAB–TolC multidrug efflux pump. *Nature* **509**, 512–515 (2014).
45. Gupta, K. *et al.* Identifying key membrane protein lipid interactions using mass spectrometry. *Nat. Protoc.* **13**, 1106–1120 (2018).
46. Pyle, E. *et al.* Structural Lipids Enable the Formation of Functional Oligomers of the Eukaryotic Purine Symporter UapA. *Cell Chem. Biol.* **25**, 840-848.e4 (2018).
47. Teo, A. C. K. *et al.* Analysis of SMALP co-extracted phospholipids shows distinct membrane environments for three classes of bacterial membrane protein. *Sci. Rep.* **9**, 1813 (2019).
48. Hopper, J. T. S. *et al.* Detergent-free mass spectrometry of membrane protein complexes. *Nat. Methods* **10**, 1206–1208 (2013).
49. Marty, M. T., Hoi, K. K. & Robinson, C. V. Interfacing Membrane Mimetics with Mass Spectrometry. *Acc. Chem. Res.* **49**, 2459–2467 (2016).
50. Reading, E. *et al.* The Role of the Detergent Micelle in Preserving the Structure of Membrane Proteins in the Gas Phase. *Angew. Chemie Int. Ed.* **54**, 4577–4581 (2015).
51. Leney, A. C., McMorran, L. M., Radford, S. E. & Ashcroft, A. E. Amphipathic polymers enable the study of functional membrane proteins in the gas phase. *Anal. Chem.* **84**, 9841–7 (2012).
52. Watkinson, T. G., Calabrese, A. N., Ault, J. R., Radford, S. E. & Ashcroft, A. E. FPOP-LC-MS/MS Suggests Differences in Interaction Sites of Amphipols and Detergents with Outer Membrane Proteins. *J. Am. Soc. Mass Spectrom.* **28**, 50–55 (2017).
53. Calabrese, A. N., Watkinson, T. G., Henderson, P. J. F., Radford, S. E. & Ashcroft, A. E. Amphipols outperform dodecylmaltoside micelles in stabilizing membrane protein structure in the gas phase. *Anal. Chem.* **87**, 1118–26 (2015).
54. Bechara, C. *et al.* A subset of annular lipids is linked to the flippase activity of an ABC transporter. *Nat. Chem.* **7**, 255–262 (2015).
55. Fahy, E. *et al.* Update of the LIPID MAPS comprehensive classification system for lipids. *J. Lipid Res.* **50 Suppl**, S9-14 (2009).
56. Hall, S. C. L. *et al.* Influence of Poly(styrene- *co* -maleic acid) Copolymer Structure on the Properties and Self-Assembly of SMALP Nanodiscs. *Biomacromolecules* **19**, 761–772 (2018).

7. Figures

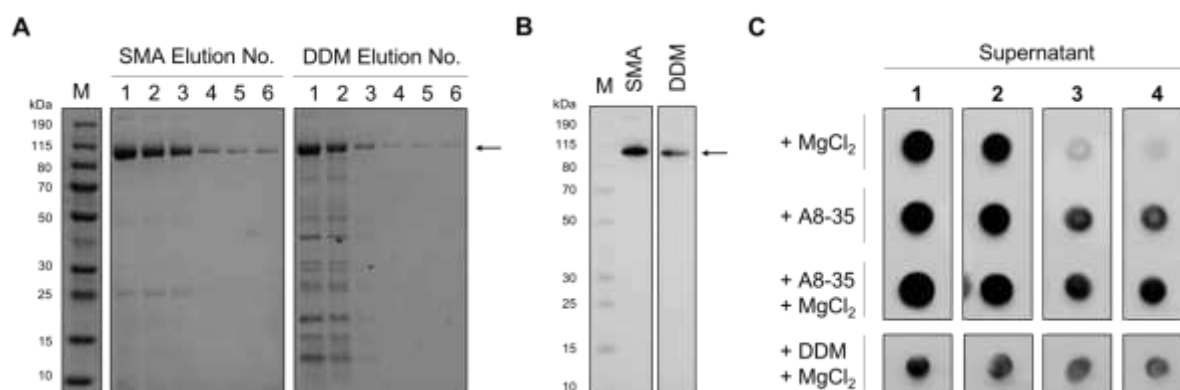


Figure 1: Solubilisation and purification efficiency of SMA vs DDM for AcrB (A and B), alongside a dot blot monitoring the exchange procedure from SMA into amphipol A8-35 and DDM (C).

A) Representative elution fractions (1-6) from a standard one-step IMAC purification of AcrB in SMA and DDM alongside molecular weight marker (M). Arrow indicates the expected molecular mass of AcrB. **B)** Anti-His western blot of final AcrB(His)₈ samples in SMA and DDM with overlaid molecular weight marker (M) prior to further experimentation. **C)** Dot blot showing the relative amount of soluble AcrB remaining in the supernatant after each incubation with the precipitant (MgCl₂), rescue agent (A8-35 or DDM), or a combination of both. Supernatant 1 represents the sample after incubation and centrifugation with the first MgCl₂ addition, in this case 0.5 mM MgCl₂. Supernatants 2-4 represent the remaining soluble AcrB after each 0.5 mM increment of MgCl₂ added to the sample. The same antibody was used as in B.

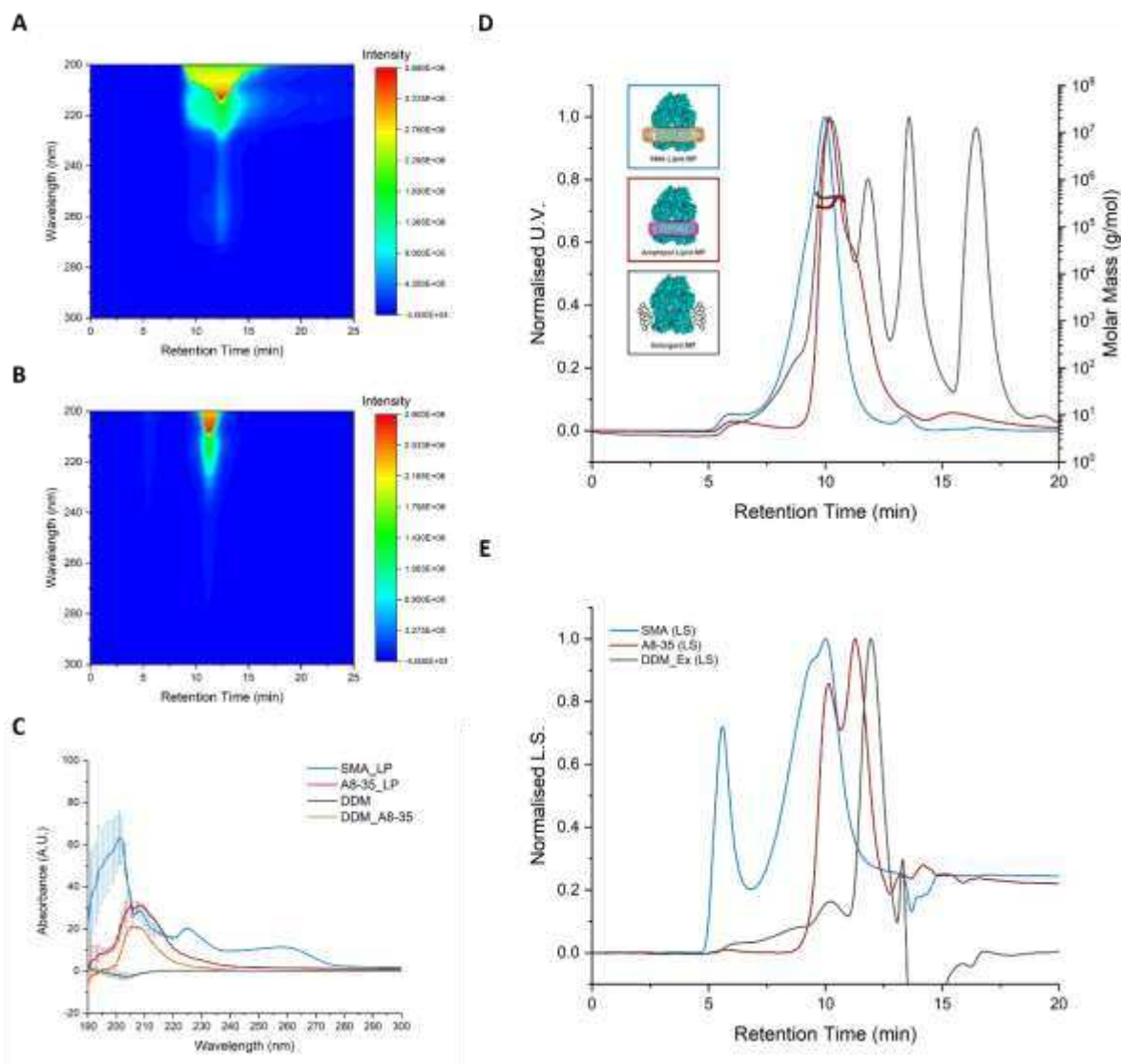


Figure 2: SEC-MALLS analysis of exchanged samples and evidence of polymer interference across a range of UV wavelengths.

A) Multi-wavelength SEC profile of protein-free SMA lipid particle (SMA_LP) in heat map representation. Relative absorbance at each wavelength is shown as intensity, ranging from highest absorbance (red) to the lowest (blue), and plotted according to retention time in minutes. **B)** As A, but with amphipol A8-35 lipid particles (A8-35_LP). **C)** UV absorbance of DDM alongside SMA_LP and A8-35_LP from A and B. A8-35 was also mixed with DDM (DDM_A8-35) to give clarification on the polymer and lipid contributions to absorbance across a range of wavelengths. Error bars represent triplicate results. **D)** SEC-MALLS chromatograms and molar mass distributions of SMA:AcxB (blue), A8-35_Ex (green) and DDM_Ex (yellow). Images representing the different solubilisation platforms from Figure 1 have been colour-coded according to their related SEC profiles. **E)** Light scattering (LS) profiles of the same samples shown in A, colour-coded according to A. Traces in A) and B) were normalized relative to the highest peak (Normalized U.V./L.S.) and plotted as a function of retention time in minutes (min).

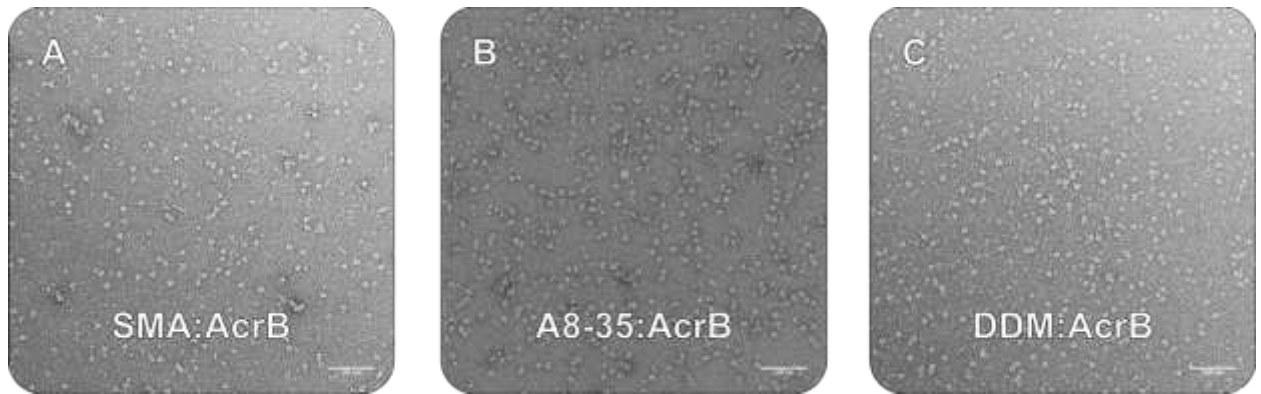


Figure 3: Negative stain analysis of AcrB after extraction in SMA and its subsequent exchange in A8-35 and DDM. Representative negative stain micrographs of SMA:AcrB before (A) and after exchange into A8-35 (B) and DDM (C). In each instance the “typical” broadly triangular shape can be seen with no significant aggregation. Micrographs were taken at 50k mag. Bottom-right scale bar = 100 nm.

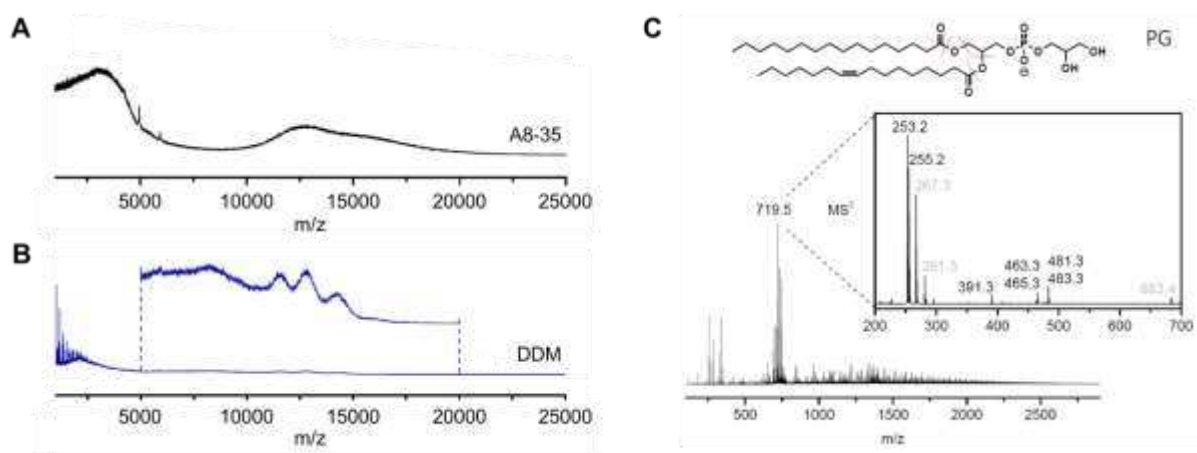


Figure 4: Mass spectrometry analysis of SMA extracted AcrB after exchange into A8-35 and DDM. Initial native MS results of A8-35_Ex (A) and DDM_Ex (B). C) Tandem mass spectra (MS/MS) of lipids extracted from A8-35_Ex, demonstrating that at least one lipid can be identified as phosphatidylglycerol (PG). The preferential fragmentation positions of PG (16:0/16:1) are indicated by red dotted lines. MS/MS-peaks which could not be explained were labelled in grey.

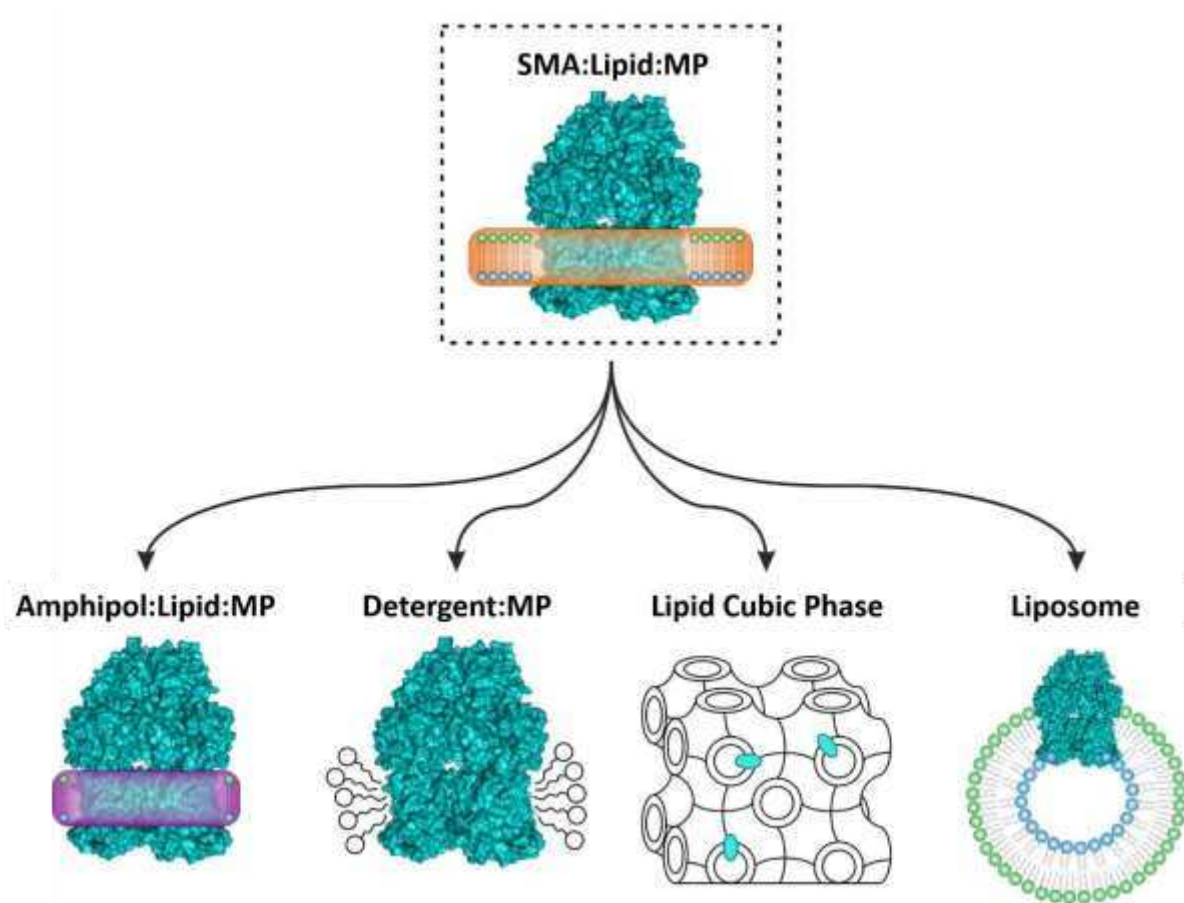
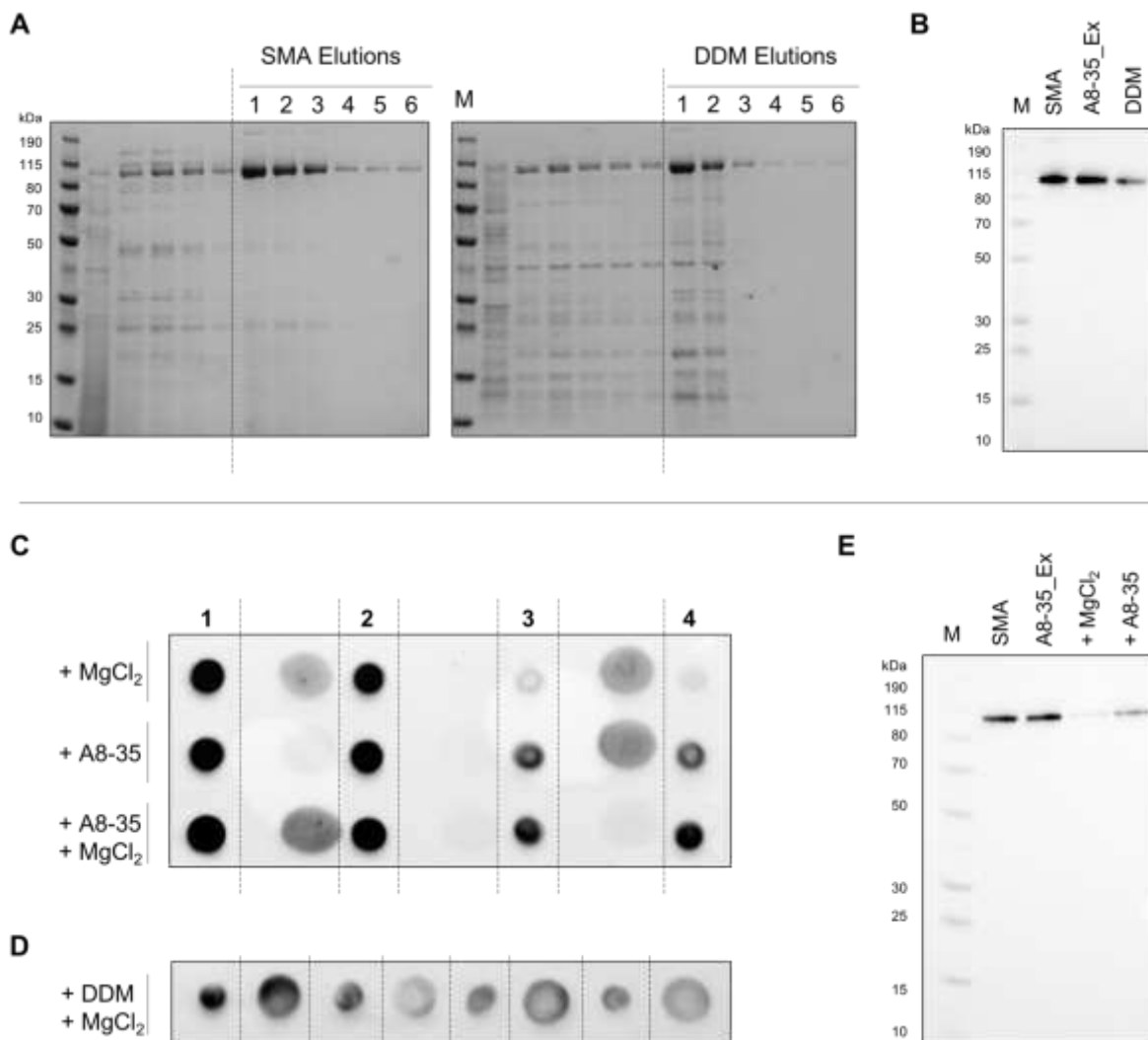


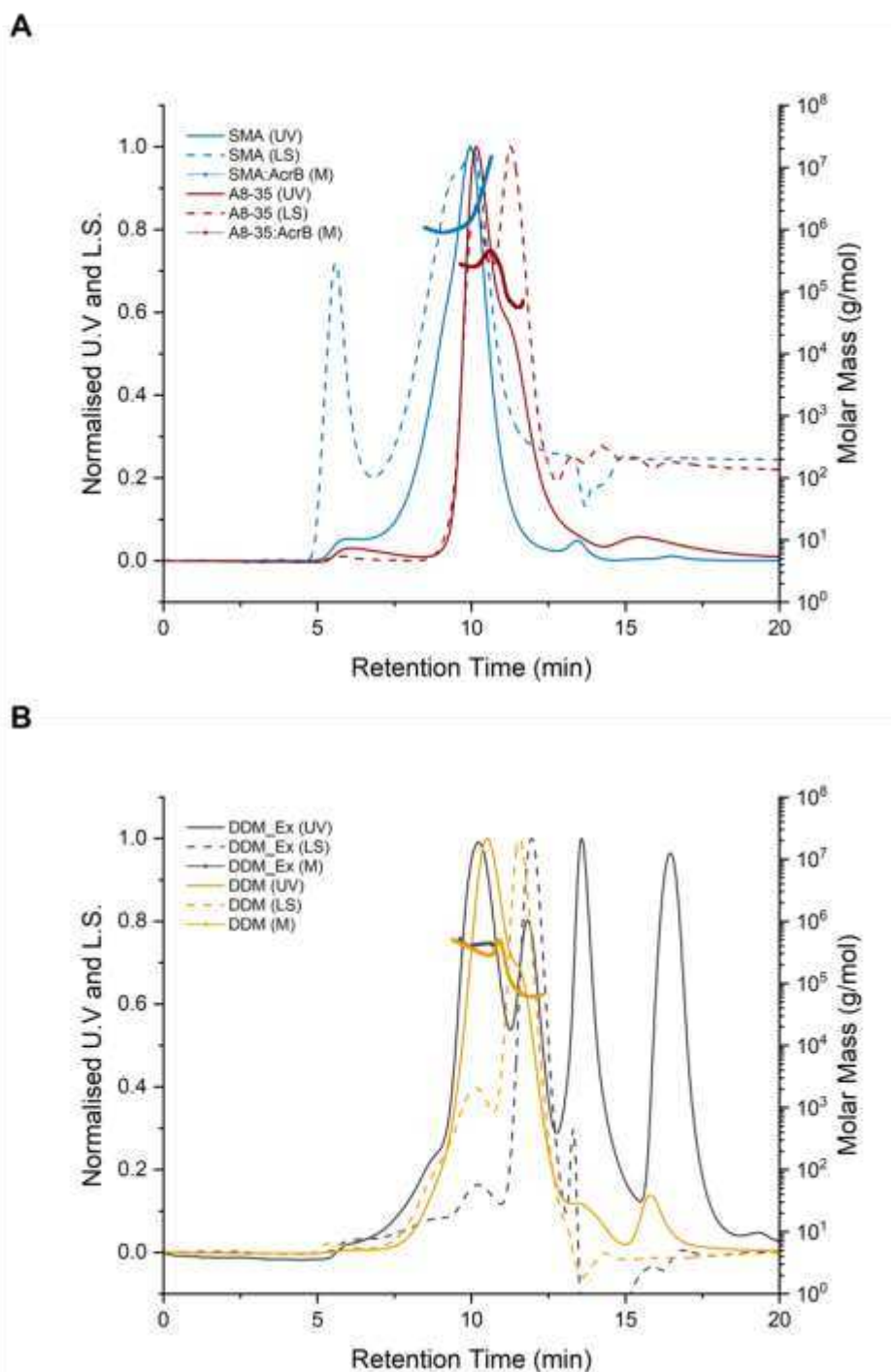
Figure 5: SMALPs as a vehicle for transfer into downstream membrane protein solubilisation platforms.

Schematic highlighting the versatility of the SMA co-polymer as a vehicle for reconstitution into downstream solubilisation platforms amphipol, detergents, lipid cubic phase and liposomes.

8. Supplementary Figures



Supplementary Figure 1: **A)** Full gel images of SMA and DDM purifications of AcrB with accompanying molecular weight markers. **B)** Full western blot image of SMA and DDM purified AcrB samples with A8-35_Ex sample in middle lane (omitted in final image in Figure 1B). **C)** Complete dot blot of amphipol A8-35_Ex samples – dotted lines represent boxed regions shown in Figure 1C. The larger regions in between represent the insoluble regions. **D)** Full dot blot of DDM_Ex samples – dotted lines represent boxed regions shown in Figure 1C. **E)** Western blot of complete exchange process showing original SMA sample (SMA), the final exchanged sample (A8-35_Ex), the MgCl₂-only control, and A8-35-only control alongside MW marker.

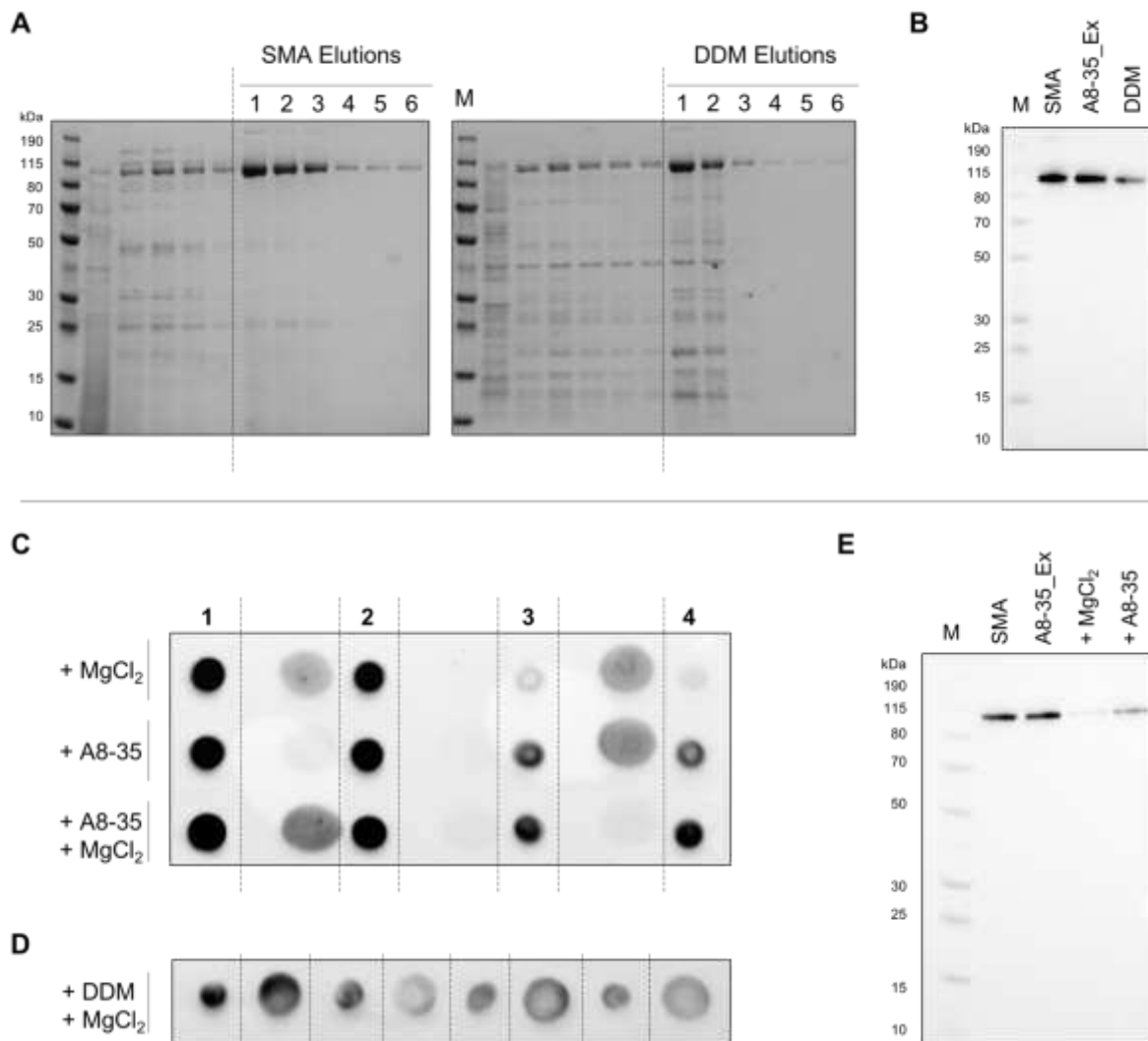


Supplementary Figure 2: **A)** SEC-MALLS analysis of SMA:AcxB (blue) and A8-35_Ex (red). Solid lines represent UV absorbance at 280 nm and dashed lines represent light scattering signal. Traces were normalized relative to the highest peak (Normalized U.V.), and plotted as a function of retention time in minutes. A refractive index increment (dn/dc) value of 0.16 mL/g from⁵⁶ was applied for SMA molar mass calculations, but there are clear issues with the calculations and this is included purely for illustrative purposes. **B)** SEC-MALLS analysis of DDM:AcxB (yellow) and DDM_Ex (grey). Solid lines represent UV absorbance at 280 nm and dashed lines represent light scattering signal. Traces were normalized relative to the highest peak (Normalized U.V.), and plotted as a function of retention time in minutes. Calculated molar mass distributions are shown across the entire peak for both samples.

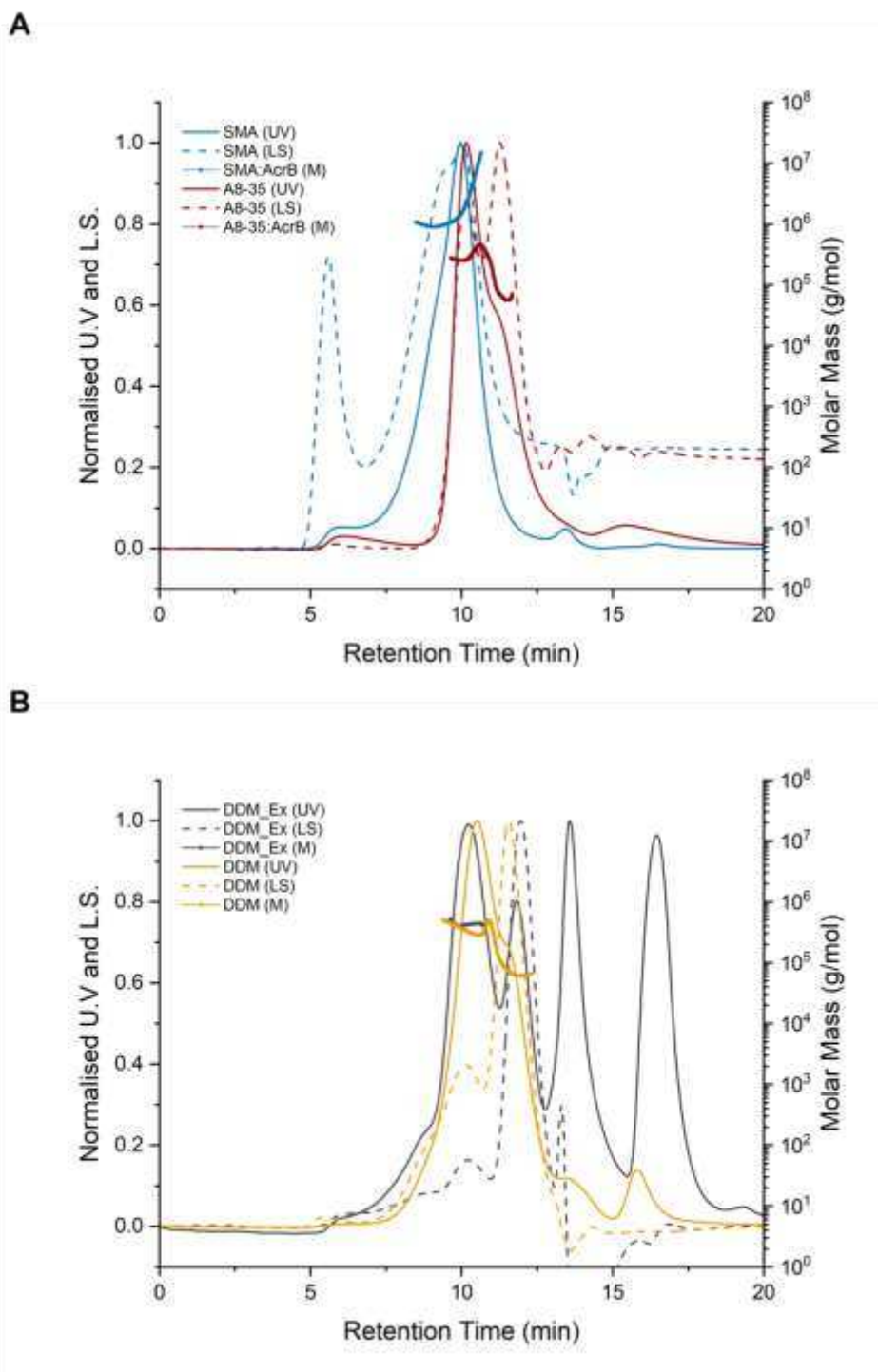
<i>Sample Name</i>	MgCl₂	A8-35	Protein Before (μg)	A8-35 Added (μg)	Protein Conc. After (mg/ml)	Protein After (μg)	Fold Reduction
<i>Control 1</i>	+	-	72.0	-	0.229	2.9	24.83
<i>Control 2</i>	-	+	116.8	350.4	0.335	41.8	2.79
<i>Sample 1</i>	+	+	116.8	350.4	0.340	42.5	2.75
<i>Sample 2</i>	+	+	116.8	350.4	0.327	40.8	2.86
<i>Sample 3</i>	+	+	196.0	588.0	0.789	73.6	2.66

Supplementary Table 1: Conditions of each sample at the start of the experiment are shown in the leftmost columns in green, where control 1 is AcrB with MgCl₂ alone, control 2 is A8-35 alone, and samples 1, 2 and 3 are repeats of the exchange experiment containing both MgCl₂ and A8-35. The final sample parameters measured after the exchange are shown in the rightmost columns in blue.

Supplementary Information



Supplementary Figure 1: **A)** Full gel images of SMA and DDM purifications of AcrB with accompanying molecular weight markers (MWM). **B)** Full western blot image of SMA and DDM purified AcrB samples with A8-35_Ex sample in middle lane (omitted in final image in Figure 1B), alongside the same MWM as in A. **C)** Complete dot blot of amphipol A8-35_Ex samples – dotted lines represent boxed regions shown in Figure 1C. The larger regions in between represent other samples. **D)** Full dot blot of DDM_Ex samples – dotted lines represent boxed regions shown in Figure 1C. **E)** Western blot of complete exchange process showing original SMA sample (SMA), the final exchanged sample (A8-35_Ex), the MgCl₂-only control (+MgCl₂), and A8-35-only control (+A8-35), alongside MWM as in A.



Supplementary Figure 2: **A)** SEC-MALLS analysis of SMA:AcRb (blue) and A8-35_Ex (red). Solid lines represent UV absorbance at 280 nm and dashed lines represent light scattering signal. Traces were normalized relative to the highest peak (Normalized U.V.), and plotted as a function of retention time in minutes. A refractive index increment (dn/dc) value of 0.16 mL/g from [1] was applied for SMA to give the molar mass distribution (shown as a line across the peak), but there were issues with the calculations and this data is included for relative comparisons of heterogeneity only. **B)** SEC-MALLS analysis of DDM:AcRb (yellow) and DDM_Ex (grey). Solid lines represent UV absorbance at 280 nm and dashed lines represent light scattering signal. Traces were normalized relative to the highest peak (Normalized U.V.), and plotted as a function of retention time in minutes. Calculated molar mass distributions are shown across the entire peak for both samples and are coloured according to each sample as described in A.

Sample Name	MgCl₂	A8-35	Protein Before (μg)	A8-35 Added (μg)	Protein Conc. After (mg/ml)	Protein After (μg)	Fold Reduction
<i>Control 1</i>	+	-	72.0	-	0.229	2.9	24.83
<i>Control 2</i>	-	+	116.8	350.4	0.335	41.8	2.79
<i>Sample 1</i>	+	+	116.8	350.4	0.340	42.5	2.75
<i>Sample 2</i>	+	+	116.8	350.4	0.327	40.8	2.86
<i>Sample 3</i>	+	+	196.0	588.0	0.789	73.6	2.66

Supplementary Table 1: Conditions of each sample at the start of the experiment are shown in the leftmost columns in green, where control 1 is AcrB with MgCl₂ alone, control 2 is A8-35 alone, and samples 1, 2 and 3 are repeats of the amphipol exchange experiment containing both MgCl₂ and A8-35. The final sample conditions measured after the exchange are shown in the rightmost columns in blue.